ACSNANO
www.acsnano.org
ARTICLE

Bicontinuous Fluid Structure with Low Cohesive Energy: Molecular Basis for Exceptionally Low Interfacial Tension of Complex Coacervate Fluids

Kuo-Ying Huang,[†,#] Hee Young Yoo,[‡,#] YongSeok Jho,[*,§,∥] Songi Han,[*,†] and Dong Soo Hwang[*,‡,⊥]

[†]Department of Chemistry and Biochemistry, University of California Santa Barbara, Santa Barbara, California 93106, United States

[‡]Division of Integrative Biosciences and Biotechnology, Pohang University of Science and Technology (POSTECH), Pohang 37673, Republic of Korea

[§]Center for Soft and Living Matter, Institute for Basic Science (IBS), Ulsan 44919, Republic of Korea

[∥]Asia-Pacific Center for Theoretical Physics, Pohang 37673, Republic of Korea

[⊥]School of Environmental Science and Engineering, Pohang University of Science and Technology (POSTECH), Pohang 37673, Republic of Korea

Supporting Information

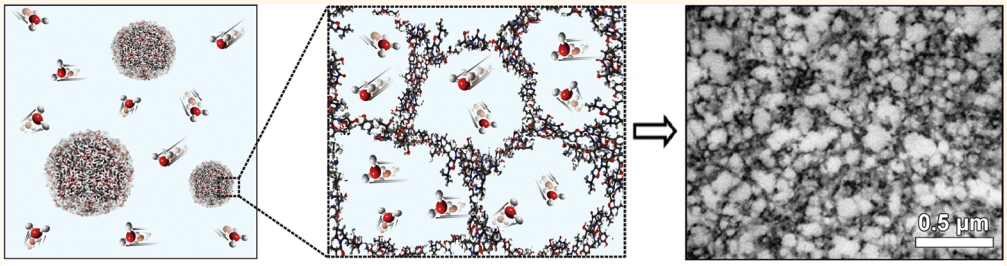

Water-filled bicontinuous nanostructured complex coacervate fluid with low cohesive energy gives rise to low interfacial tension

ABSTRACT: **An exceptionally low interfacial tension of a dense fluid of concentrated polyelectrolyte complexes, phase-separated from a biphasic fluid known as complex coacervates, represents a unique and highly sought-after materials property that inspires novel applications from superior coating to wet adhesion. Despite extensive studies and broad interest, the molecular and structural bases for the unique properties of complex coacervates are unclear. Here, a microphase-separated complex coacervate fluid generated by mixing a recombinant mussel foot protein-1 (mfp-1) as the polycation and hyaluronic acid (HA) as the polyanion at stoichiometric ratios was macroscopically phase-separated into a dense complex coacervate and a dilute supernatant phase to enable separate characterization of the two fluid phases. Surprisingly, despite up to 4 orders of magnitude differing density of the polyelectrolytes, the diffusivity of water in these two phases was found to be indistinguishable. The presence of unbound, bulk-like, water in the dense fluid can be reconciled with a water population that is only weakly perturbed by the polyelectrolyte interface and network. This hypothesis was experimentally validated by cryo-TEM of the macroscopically phase-separated dense complex coacervate phase that was found to be a bicontinuous and biphasic nanostructured network, in which one of the phases was confirmed by staining techniques to be water and the other polyelectrolyte complexes. We conclude that a weak cohesive energy between water−water and water−polyelectrolytes manifests itself in a bicontinuous network, and is responsible for the exceptionally low interfacial energy of this complex fluid phase with respect to virtually any surface within an aqueous medium.**

KEYWORDS: *complex coacervate, interfacial energy, cryo-transmission electron microscopy, Overhauser effect dynamic nuclear polarization, hydration water, water dynamics, polyelectrolyte complexes*

For sessile marine organisms like mussels to survive in a robust wave environment under water, they secrete high concentration of water-soluble adhesive polyelectrolytes containing, among others, the catecholic functional group of

Received: December 11, 2015
Accepted: May 6, 2016

DOI: 10.1021/acsnano.5b07787
ACS Nano XXXX, XXX, XXX−XXX

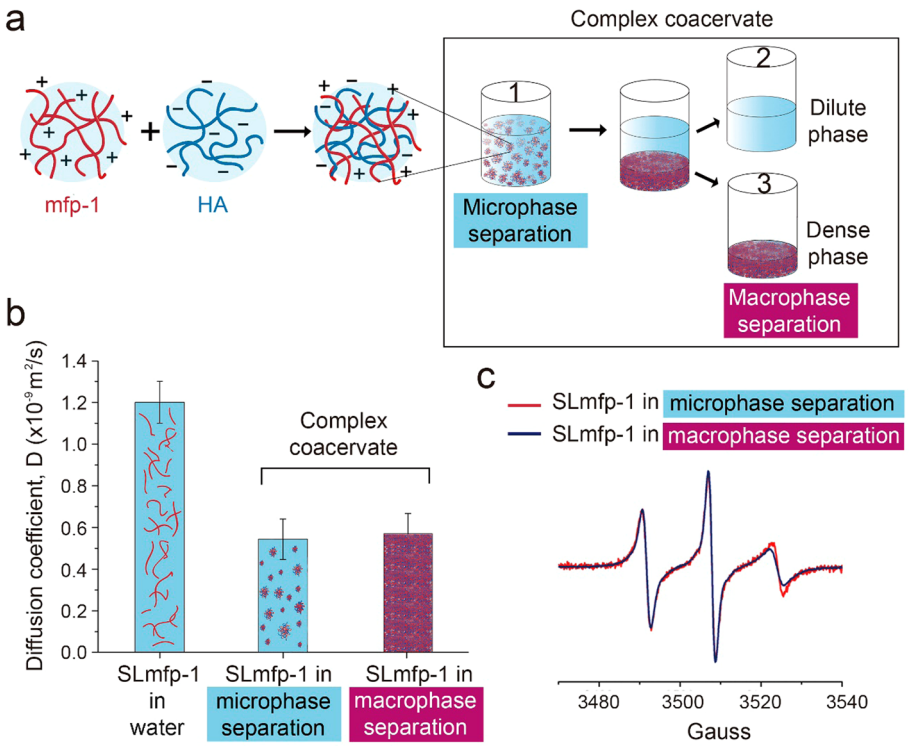

Figure 1. (a) Schematics of complex coacervation of mfp-1 and hyaluronic acid (HA): (1) complex coacervate suspension; (2)dilute phase; (3) dense phase of coacervate. (b) Translational diffusion coefficients of mfp-1 hydration in coacervated state. We find that mfp-1 hydration dynamics are similar whether coacervates exist as suspension droplets or as dense phase coacervate after a macro phase separation. These results suggest that mfp1 does not alter its conformation as a result of the macro-phase separation. (c) EPR spectra of spin labeled mfp-1 (SLmfp-1) in suspension coacervate droplets (red) and in dense phase coacervates.

3,4-L-dihydroxyphenylalanine (DOPA) that adhere strongly to wet metal oxide surfaces.[1,2] When the organism secretes the ingredients of the to-be-waterproof-adhesive, this water-soluble polymer cocktail composed mainly of polyelectrolytes would remarkably stay where it is placed on the metal oxide surface without being dissolved and dissipated into the ocean; the most compelling and current model is that this is achieved by exploiting a molecular assembly mechanism known as complex coacervation.[3,4]

Complex coacervation is a fluid−fluid phase separation which occurs when two oppositely charged polyelectrolytes neutralize each other and form microdroplets of nanometers up to tens of micrometers in size, suspended in a supernatant solution devoid of polyelectrolytes, henceforth referred to as microphase separation[5,6] (Figure 1a). At a given range of pH, temperature, and concentration, the two polyelectrolytes form solution complexes (Schematic 1 in Figure 1a), coalesce into a growing mass, and eventually separate into a highly dense fluidic phase (Schematic 3 in Figure 1a). This polyelectrolyte-rich dense phase is called the "complex coacervate" and exhibits suitable physical properties as an underwater adhesive for sessile marine organisms, such as high fluidity, low interfacial tension, and high polymer density of the adhesive polyelectrolytes.[3,4,7]

Complex coacervates, whether formed by polymer or protein based polyelectrolytes, are signified by a highly peculiar physical property of displaying an extremely low interfacial tension $\gamma \equiv (\partial G/\partial A)_{T,P}$, where G is the Gibbs free energy, $A$is the area, T is the temperature, and P is the pressure. This interfacial tension, γ, of the coacervate phase is low relative to virtually any solid surface under water,[8−11] which is a core feature of the coacervate phase as an intermediary for the adhesion of marine mussels, as they readily coat a wide range of surfaces without escaping to the aqueous bulk solution. This property is particularly crucial for the coating of a rough surface, where a molecularly even contact between the substrate surface and the coacervate fluid cannot be achieved by simply applying pressure with a fluid displaying high interfacial tension with contact angles on the order of or larger than that of the substrate roughness. If the multicomponent solution of adhesive proteins that forms a complex coacervate has high interfacial tension, instead of molding around the rough surface, it will form water bubbles between them and the rough surface, reducing their adhesive ability (see Supporting Information Figure S1). The utility of installing low interfacial tension property to the polymer solution of interest is immediate and broad, benefiting drug delivery and non-carbon paper ink to the delivery of flavor ingredients, to name just a few technological application.[6] To date, however, it is unclear what the design principle for achieving lower surface tension is for a given synthetic adhesive fluid, because the molecular basis and tuning parameters for the exceptionally low surface tension of the coacervate phase is not fully understood and intensively debated,[4,5,11−14] shedding light on this is our main objective.

The interfacial tension of the coacervate phase is low relative not only to most solid surfaces, but also to water, as has been observed by Atomic Force Microscopy (AFM)[8,14] and Surface Forces Apparatus (SFA) measurements,[4,9] and results in the growth of the coacervate phase well beyond molecular dimensions of the polyelectrolyte constituents.[8] Interestingly, the low interfacial energy of the coacervate phase relative to water measurably decreases when salt concentration is increased,[8,10,11,13,15] suggesting that the strength or weakness

DOI: 10.1021/acsnano.5b07787
ACS Nano XXXX, XXX, XXX−XXX

of polyelectrolyte−polyelectrolyte and/or polyelectrolyte−water interactions of electrostatic origin is a key modulator of the interfacial tension of the coacervate phase. Corroborating reports in the literature include that changes of the salt concentration or the polycation/anion ratio have the most significant effect on the complex coacervate composition, including water content.[16] The core objective of this study is to test the hypothesis that the exceptionally low interfacial energy of the complex coacervate phase is directly rooted in the low cohesive energy of the complex coacervate phase, and not in a strong attractive energy between the complex coacervate fluid phase and the surrounding surfaces. In the latter case, the interfacial energy would inevitably depend sensitively on the specific surface at hand, although coacervate−surface attraction may well be an additional factor in determining the interfacial tension of the coacervate phase.

As the complexation and coacervation of two oppositely charged polyelectrolytes occur at carefully tuned and relatively high ionic strength (typically NaCl concentration of 500 mM), the electrostatic field of the polyelectrolyte complex is largely or partially screened, exposing a less charged and less hydrophilic polymer backbone to the solvent compared to in low ionic strength solution. The local charge neutrality shields the propagation of the electric field beyond the dimensions of the polyelectrolyte complexes that will include sandwiched hydration water. As a result, only water within a few angstrom distance from the polyelectrolyte framework will experience a weakened electric field, and will therefore experience less cohesion than hydration water coupled to a highly charged polyelectrolyte surface. Here, it is important to point out that there is consensus in the literature that the dense complex coacervate fluid phase is highly populated with dynamic water with reports ranging from 60 to above 80 wt %.[16−18] Recent reports that the nonfreezing water content is maximized within coacervated fluids are also noteworthy in this context.[19] When water is not strongly coupled by electrostatic interactions to the polyelectrolyte complex surfaces, its separation from the polyelectrolytes does not incur a high energetic penalty and its cohesive energy with the rest of the water is lower. In fact, the cohesive energy of this dynamic water can be lower than that of bulk water, if the interaction between water and the polyelectrolyte complex surfaces is comparable with or weaker than the water−water interaction in bulk, so that the polyelectrolyte complexes effectively perturb, not strengthen, the surrounding water structure. This property, the less favorable polyelectrolyte complex−water and water−water interaction energy of the complex coacervate phase, will lower the interfacial tension between the complex coacervate fluid phase and a solid surface at a given adhesion energy between the coacervate fluid phase and the surface. In contrast, if the water is strongly bound to the polyelectrolyte surfaces, it is energetically costly to remove the hydration layer from the polyelectrolyte surfaces. This dehydration process is critical because for the polyelectrolyte to coat and adhere to a solid surface under water, its hydration layer needs to be first displaced, before adhesive contact between the polymer and the solid surface can be established to fully exploit the adhesion interaction exerted by the surface chemistry of the polyelectrolytes or the solid. Thus, the more favorable polyelectrolyte complex−water and water−water interaction will increase the cohesive energy of the complex coacervate phase and increase the interfacial tension between the complex coacervate fluid phase and a solid surface

So, while the notion of weakly cohesive water within the dense complex coacervate phase can be logically reconciled with observations in the literature of finding high populations of water, and this water to be freely diffusing within a highly dense fluidic polymer phase,[16−18] as well as the low interfacial tension with respect to water[9] and solid surfaces, a more direct observation of this property is desirable. Here, we remind the reader that the cohesive energy of water—bulk, interstitial or interfacial—is reflected in the translational diffusivity of water, if the water population of interest can be selectively measured. Thus, the stronger the diffusion retardation, the stronger the cohesive energy of the water in the absence of physical confinements, *i.e.* in free solution, and *vice versa*.[20] This is our rationale for pursuing the measurement of the diffusivity of internal water interacting within the dense complex coacervate phase. The translational diffusivity of water within the local volume or near the surface of interest was measured by an established method of ^{1}H Overhauser dynamic nuclear polarization (ODNP) at 0.35 T magnetic field by exploiting nitroxide radical-based spin probes included in the solution volume of interest or spin labels tethered to the polymer surface of interest.[17,20−22] The rotational mobility of these spin probes or labels was concurrently evaluated by continuous wave (cw) electron paramagnetic resonance (EPR) line shape analysis of the same samples. In parallel to these spectroscopic measurements of molecular-level properties, the ultrastructural property of the dense, phase-separated, complex coacervate phase was examined by cryo-TEM and differential staining, and the interfacial energy of this fluid was measured by the pendant-drop method. These set of characterization of molecular-level and macroscopic properties were applied to the macroscopically phase-separated complex coacervate phase, while deliberately modulating the polyelectrolyte−water interaction in the coacervate phase by the addition of PEG that is a known viscogen that attracts a strong and robust hydration layer.[23]

Our experimental design is aimed at addressing the following questions: Can we experimentally identify and verify exceptionally weak polyelectrolyte−surface water and water−water interaction in the dense complex coacervate fluid phase? If so, what are the structural and dynamic properties of the coacervate materials that give rise to a fragile network of interstitial water? Will in turn the factors that modulate the polyelectrolyte−surface water and water−water attraction concurrently modulate the interfacial tension of the coacervate fluid phase?

RESULTS AND DISCUSSION

Macroscopic Phase Separation of Complex Coacervate Fluid into Dense Complex Coacervate Fluid and Supernatant. Positively charged recombinant mussel foot protein-1 (mfp-1)[24,25] and negatively charged hyaluronic acid (HA) were mixed to generate complex coacervate samples (Figure S2). Complex coacervation, of mfp-1 and HA resulting in a fluid−fluid microphase separation into polymer-dense microdroplets of nanometers up to tens of micrometers size suspended in a dilute polymer-depleted solution, was found to be maximal at a weight ratio of 55:45 where their net charge neutralization is expected (Figure S3). Therefore, mfp-1/HA complex coacervates were prepared by mixing mfp-1 and HA solution at the mass ratio of 55:45 with the total polymer concentration of 2% (w/v) at pH 5.0 and 10 mM acetate buffer. After the complex coacervate fluid was formed, spin probes were introduced into the microphase-separated coacervate

DOI: 10.1021/acsnano.5b07787
ACS Nano XXXX, XXX, XXX−XXX

suspension and equilibrated (schematic 1 in Figure 2a). This complex coacervate suspension was then macrophase-separated

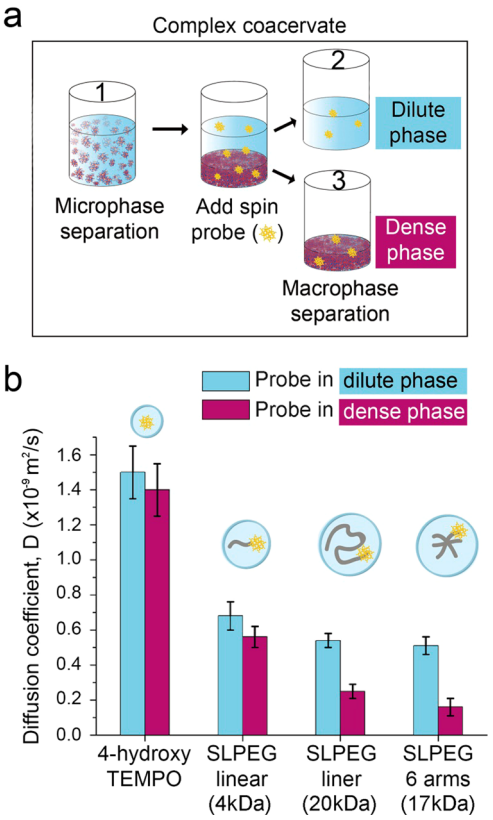

Figure 2. (a) Schematics of the spin probe added complex coacervation of mfp-1 and hyaluronic acid (HA) and (b) translational diffusion coefficients of water in the dilute and dense phases of complex coacervates (light blue and purple, respectively) using different size spin probes. The water diffusion coefficient inside the dense phase coacervates is similar to that inside the dilute phase when we use 4-hydroxy TEMPO as a spin probe. When we use large spin labeled PEG (SLPEG) as a spin probe, the diffusion dynamics of PEG surface water slow down 2- to 3-fold inside the dense phase coacervates compared to those seen in the dilute phase coacervates.

in order to separately characterize the property of the pure dilute supernatant (schematic 2 in Figure 1a) *vs* the dense complex coacervate phase (schematic 3 in Figure 1a), achieved by a combination of slight centrifugation (2000*g* for 10 min) to facilitate the phase separation or by waiting for a day. The total density of the polyelectrolytes of the mfp-1/HA coacervate in the dilute (schematic 2 in Figure 1a) and the dense phase (schematic 3 in Figure 1-a) as determined by an amino acid analyzer was ∼0.1 and 1000 mg/mL, respectively. For the concurrent characterization by ODNP and EPR of the microphase-separated complex coacervate suspension *vs* the macrophase-separated dense complex coacervate fluid and the dilute supernatant, different spin probes are employed, namely nitroxide spin labels covalently attached to the polycation mfp-1 (Figure S2), the free and hydrophilic spin probe, 4-hydroxy (4OH) TEMPO, as well as spin labels covalently attached to polyethylene glycol of varying sizes or shapes. In addition, the dense complex coacervate fluid phase was separately characterized by TEM and the measurement of interfacial tension.

Bulk-like Water Diffusivity in Dense Complex Coacervate Fluid. ODNP reports on instantaneous water diffusivity in the tens to hundreds of picosecond time scale within 5−10 Å of a stable nitroxide-based spin probe (provided changes in the spin probe's solvent accessibility are taken into account), and thus on the cohesiveness of the water network near the local spin probe of interest, the subject of our interest.[17,20−22] For the purpose of separately studying the macrophase-separated dense complex coacervate fluid and the dilute coacervate supernatant, the water-soluble and hydrophilic spin probe, 4OH TEMPO, was dissolved in the respective fluid for their characterization. In contrast, spin probes covalently attached to the mfp-1 protein surface were used to probe the diffusivity of hydration water near mfp-1, the polycation, as incorporated in the complex coacervate droplet, allowing us to study the hydration water dynamics within the dense complex coacervate microphase, without needing to macroscopically phase-separate the complex coacervate suspension.

First, we compare the ODNP-derived diffusivity of water near the surface of spin labeled mfp-1 (SL-mfp-1) in 10 mM sodium acetate buffer at pH 5.0 in dilute solution *versus* in the complex coacervate phase formed in the same buffer solution. The water diffusivity within the dense complex coacervate prior to phase separation in the microphase (schematic 1 in Figure 1a) and in the macrophase upon phase separation (schematic 3 in Figure 1a) was separately monitored.

The ODNP-derived diffusivity of hydration water on the surface (within 5−10 Å) of the SL-mfp-1 in bulk water, in the complex coacervate microphase, and in the dense coacervate macrophase are found to be 1.2×10^{-9}, 5.6×10^{-10}, and 5.8×10^{-10} m^2/s, respectively (Figure 1b). In other words, the diffusivities of the SL-mfp-1 in the complex coacervate phases before (dotted cyan column) *vs* after macrophase-separation (purple column) are identical within error (Figure 1b). Because the spin probe is covalently conjugated on the surface of the mfp-1 protein, the value for hydration dynamics as measured by SL-mfp-1 represents the hydration water diffusivity of mfp-1 as complexed within the dense complex coacervate microphase (the droplet size of the dense coacervate fluid with hundreds of nanometers to few micrometers well exceeds molecular dimensions). In fact, this is verified by our observation of indistinguishable diffusivity values on the surface of SL-mfp-1, whether as part of the dense coacervate microphase or macrophase. Importantly, these values are in agreement with prior reports of ODNP-derived surface water diffusivity on spin labeled mfp-151, a related protein to mfp-1, as complex coacervated within microphase-separated droplets.[24] Another noteworthy observation is to find the diffusion retardation of water on the surface of the mfp-1 protein in the dense coacervated state relative to that in bulk water to be only 2-fold, despite dramatically differing polyelectrolyte density by up to *4 orders of magnitude*. The cw EPR line shape confirms that the spin label is mobile with a rotational correlation time of 1−2 ns, characteristic of a label tethered to a solvent-exposed protein or polymer surface (Figure 1c). Taken together, the spin label reports on typical water and protein dynamics characteristic of an isolated protein hydrated in dilute solution state, even though the dense complex coacervate microphase environment is highly crowded by an extremely high polymer density of ∼1000 mg/mL. This implies that mfp-1 is fully hydrated and nonaggregated even within the dense coacervate fluid, such that the surface water of mfp-1 is nearly invariant when densely

DOI: 10.1021/acsnano.5b07787
ACS Nano XXXX, XXX, XXX−XXX

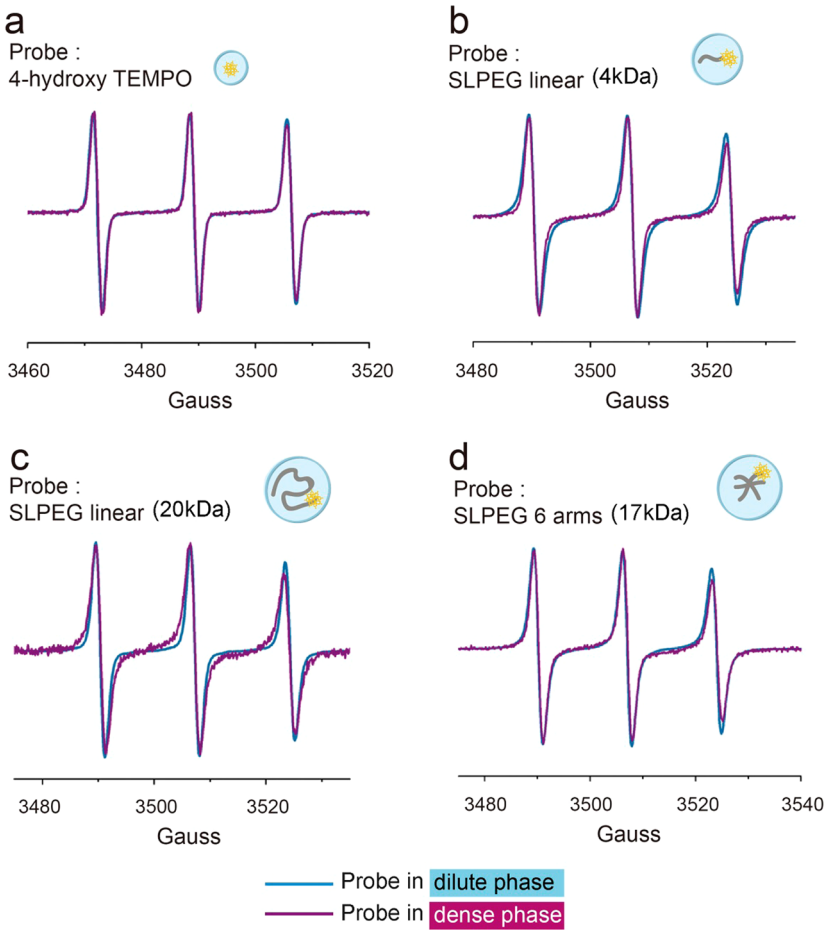

Figure 3. EPR spectra of 4 spin probes (4-hydroxy TEMPO, and spin label PEG (SLPEG) with different sizes) inside dilute phase and dense phase coacervates (light blue and purple, respectively).

crowded by polyelectrolyte complexes within the coacervate microphase. Such observation begs for further investigations.

Next, the diffusivity of interstitial water inside the phase-separated dense coacervate fluid (schematic 2 in Figure 2) and dilute coacervate supernatant (schematic 3 in Figure 2) were measured by free 4OH TEMPO spin probes. Again surprisingly, the diffusivity of water inside the dense coacervate fluid was found to be indistinguishable from that in the dilute supernatant, as shown in Figure 2 (first left histogram). This suggests that the cohesiveness of the hydrogen bond network of the water phase in the dense complex coacervate fluid as probed by 4OH TEMPO is comparable to that in the dilute supernatant, *i.e.*, effectively bulk water. In other words, there is no evidence for enhanced water−water or polymer−water attraction within the dense coacervate fluid that would manifest itself in retarded interstitial water dynamics, nor is there significant confinement effects felt by 4OH TEMPO inside the dense coacervate fluid. As for the polymer−water interaction, it collectively refers to all attractive interactions between the HA or mfp-1 surface and water. This includes electrostatic interactions between the carboxyl group of HA and other charged amino acid groups of mfp-1 and water, and H-bonding interactions between nonionic groups of HA and the protein chain, such as hydroxyl groups, *etc.*, with water. We conclude that 4OH TEMPO and water freely diffuse through a connected, bulk water-like, medium found within the phase-separated, dense, complex coacervate phase.

We supplement the ODNP results with measurements of the EPR line-shape that is sensitive to the rotational dynamics of the nitroxide spin label. Again, the EPR spectra of 4OH TEMPO inside the dense coacervates fluid and the dilute supernatant are indistinguishable in representing complete rotational freedom (shown in Figure 3a), corroborating the finding that 4OH TEMPO reports on bulk water-like properties inside the dense complex coacervate fluid.

Nanophase Separation of the Dense Complex Coacervate into a Biphasic Fluid. The observation of bulk-like water dynamics and a bulk-like local microviscosity in the vicinity of 4OH TEMPO dissolved in the dense (∼1.7 g/mL), polymer-rich (>1000 mg/mL), complex coacervate fluid phase can be reconciled with the occurrence of nanophase separation within this macrophase into polyelectrolyte-rich and dilute solution nanophases, at length scales significantly smaller compared to the coacervate fluid microdroplet size. To test this hypothesis and obtain clues about the involved length scales, we turn to cryo-TEM of the macrophase-separated dense complex coacervate phase. The cryo-TEM experiments are combined with differential staining using a contrast agent osmium oxide (OsO_4), where the area with higher polymer density displays darker contrast than the area devoid of polymer, given that OsO_4 was chosen as a contrast agent that selectively binds to the polymer surface. Intricate solution structures within the dense coacervates phase have been observed by cryo-SEM and cryo-TEM.[4,26−29] Depending on the shape and functional groups of the polyelectrolytes,

DOI: 10.1021/acsnano.5b07787
ACS Nano XXXX, XXX, XXX−XXX

different coacervate-internal solution structures seem to self-assemble. For example, a sponge-like bicontinuous solution structure within the dense complex coacervate composed of extended polyelectrolytes that mfp-1 and HA of this study also belongs to has been reported on in the literature,[4,26,29] as well as interconnected corona-like structures in coacervate composed of polyelectrolyte and micellar assemblies.[27,29] The images, as presented in Figure 4a, indeed find the presence of a heterogeneous structure of an interconnected, bicontinuous network.[4] The largest length scale for the nanophases is in the 100 nm range, while phase boundaries at smaller length scales coexist; this is what we refer to as nanophase separation into a water-filled sponge structure. According to the ODNP and EPR results, one of the main nanophases is a bulk water-like phase, leaving the other phase to be rich of polyelectrolyte complexes composed of the negatively charged HA and the positively charged mfp-1 protein.

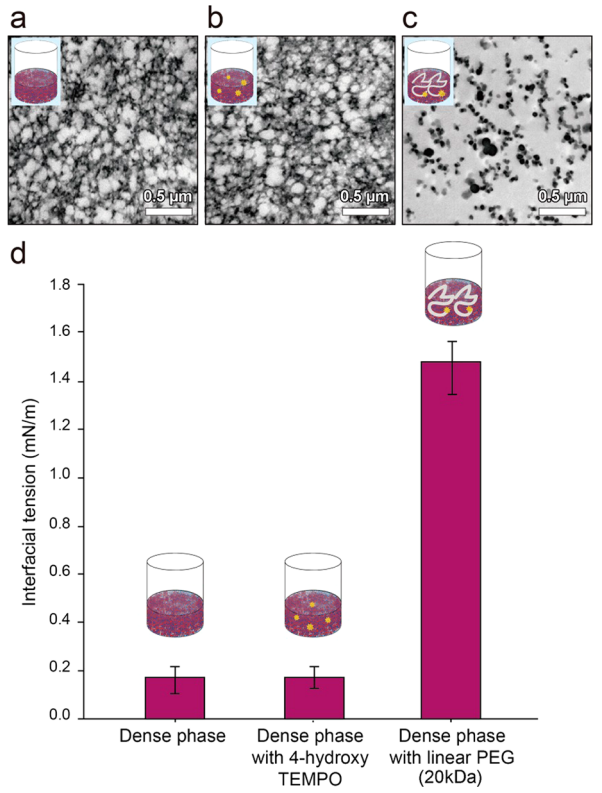

Figure 4. Structures of coacervated mfp-1/HA under a transmission electron microscope when (a) mfp-1 and HA were mixed in 55:45 (w/w) ratio, (b) mfp-1 and HA were mixed in 55:45 (w/w) ratio including 120 mM 4-hydroxy TEMPO and (c) mfp-1 and HA were mixed in 55:45 (w/w) ratio including 20 kDa PEG. The horizontal bar represents 0.5 μm. (d) Interfacial tension of mfp-1 and HA coacervated state. mfp-1 and HA were mixed in 55:45 (w/w) ratio, including 4-hydroxy TEMPO and 20 kDa PEG. (Inset: schematic of coacervated mfp-1/HA for each analysis. Each value and error bar is the mean of sextuplicate sample and its standard deviation.

Important corroborating clues are obtained when examining the fractions or solution capacities of these nanophases as derived from the partitioning of different spin probes between the dilute supernatant and the dense complex coacervate fluid phases from the double integration of the EPR spectra of these macro-phase separated fluids. When employing 4-hydroxy TEMPO as spin probes, we find twice the concentration of spins in the dilute supernatant (schematic 2 in Figure 2) compared to that in the dense coacervate fluid (schematic 3 in Figure 2) per unit volume of fluid, suggesting that the water content inside the dense coacervates is about 50% (v/v), assuming the solubility of 4-hydroxy TEMPO in the coacervate nanophase water pool is similar to that in the dilute coacervate supernatant (Table 1). This finding is consistent with the complex coacervate being a biphasic fluid with water constituting one of the main fluid nanophase, as further confirmed with the image analysis from cryo-TEM (see Figure S4).

Table 1. Spin Probe Distribution between Dilute and Dense Phase Coacervates Depends on Type and Size of the Spin Probes

spin probe	spin probe distribution between two phases[a] (dilute phase:dense phase)
4-hydroxy TEMPO	2:1
SLPEG linear (4 kDa)	6:1
SLPEG linear (20 kDa)	15−20: 1
SLPEG 6 arms (17 kDa)	∼20:1

[a]Spin probe distribution was determined by double integral of EPR signal.

Even though the finding that highly mobile, bulk-like, water coexists in a fluid containing high concentrations of highly charged polyelectrolyte complexes may seem unintuitive, this is consistent with literature reports and appears to be a key characteristic of complex coacervate fluids.[16−18] In the paper of Kausik *et al.*,[17] as well as Ortony *et al.*,[24] the surface water diffusivity of one of the polyelectrolytes, positively or negatively charged, was found to slow upon complex coacervation. However, the retardation factor for water dynamics was surprisingly modest, displaying an overall minimally hindered diffusivity of local water hydrating the polyelectrolyte surface. These findings were interpreted as the dense complex coacervate fluids being water-rich and containing bulk-like water pools.

It is important to note that the mfp-1 protein itself, embedded in the dense complex coacervate fluid, as part of microphase droplets or from macrophase-separation, is also mobile and fully hydrated, and displays characteristic of a hydrated and freely diffusing protein in dilute solution. This shows that not only are the water−water and water−polymer interaction weak, as reflected in minimal diffusion retardation for water, but also are the interactions within the polymer or between polymer complexes of the complex coacervate fluid, water mediated or not.

Weak Cohesive Energy of the Complex Coacervate Fluid. Next, we ask whether we can derive from the experimental observation reported so far clues about the molecular basis of the low interfacial tension of complex coacervate fluid. Crucially, the interfacial tension between the complex coacervate fluid and the surrounding medium is exceptionally low, not only with respect to water, but also with respect to virtually any solid surface under water. This implies that the cohesive energy of the complex coacervate fluid itself must be exceptionally low, especially as the lower interfacial tension of the complex coacervate fluid is rather universal. If so, what could be the structural basis for a lower cohesive energy of a water-rich and dense polymer solution compared to water, especially considering that the constituents of this complex fluid

DOI: 10.1021/acsnano.5b07787
ACS Nano XXXX, XXX, XXX−XXX

are highly charged polyelectrolytes? A nanophase separation between a polyelectrolyte-rich and a water phase at length scales much smaller than the dimensions of the dense coacervate droplet alone can explain the low interfacial tension between the dense complex coacervate fluid and water, as discussed in the literature.[24] However, the lower interfacial tension of the complex coacervate fluid than pure water with respect to a wide range of solid surfaces implies that the cohesive energy within the complex coacervate fluid must be significantly lower than that in bulk water. Thus, there is an additional factor that must be weakening the water−water and water−polymer interaction. First off, as the complexation and coacervation of two oppositely charged polyelectrolytes occur at carefully tuned and relatively high ionic strength, the electrostatic field of the polyelectrolyte complex is partially screened, exposing a less charged and less hydrophilic polymer backbone than in low ionic strength solution. The electrostatic complexation of these partially screened and oppositely charged moieties of the polymers effectively shields residual excess charges upon structural rearrangement and complexation of the oppositely charged polyelectrolytes at an approximately 1:1 molar stoichiometry.[4,24] This results in the exposure of effectively charge-neutral polyelectrolyte complexes to water, of which 50% of the amino acid residues of mfp-1, tyrosine and proline, are rendered hydrophobic according to the hydropathy index of Tanford and Nozaki,[30] once the positively charged lysines are shielded.[1,24] Still, what holds the coacervate phase together is primarily and most importantly the electrostatic interaction between the polycations and polyanions. Additional van der Waals or other attractive interactions between the polymer and protein-based polyelectrolytes contribute to an even stronger cohesive interaction. In any case, in this scenario, the network interaction between surface water and the extended, effectively hydrophobic or less hydrophilic, polyelectrolyte complexes is expected to be weak.[31] However, it is challenging to directly prove weak interactions between polymer complexes and water, unless we had observed faster surface water diffusivity than in bulk water. Especially in a heterogeneous fluid, the population of such fast diffusing water at the polymer−water interface will inevitably coexist with bulk-like water and water stably hydrating the charged segments of the polyelectrolyte surfaces, making it exceedingly difficult to separately observe weakly bound water populations, even if they make up a significant population.

Thus, we devise an experimental plan to test the existence of weakly adhesive and cohesive water by adding polyethylene glycol (PEG) as a copolymer that has been shown to exert strong polymer−water attraction, resulting in PEG corralling an extended hydration shell, away from the bulk-like water population.[23] The question is whether this will lead to the slowing of water diffusivity in the dense complex coacervate fluid, and more importantly, whether this will consequently change the surface tension of the complex coacervate fluid, as can be measured by its interfacial tension with respect to water. We add three different types of spin labeled PEG polymers to the macrophase-separated complex coacervate phase (Figures 1a−3), a small 4 kDa PEG spin labeled at both ends, a 20 kDa PEG spin labeled at both ends, and a 17 kDa 6-arm PEG spin labeled at all 6 arms. For reference, we will first discuss the ODNP results of freely dissolved spin labeled PEG in the dilute supernatant phase (Figure 2a) at very low polyelectrolytes concentrations. As expected and verified in previous studies,[24] the diffusivity of water near the spin label tethered to the PEG chain-end ranges from 0.5×10^{-9} to 0.7×10^{-9} m^2 s^{-1} and decreases with increasing PEG size (cyan columns in Figure 2), corresponding to retardation factors of 2- to 3-fold compared to water near free spin probes such as 4OH TEMPO, signifying the presence of a retarded water network hydrating the PEG surface (Figure 2). These values are typical of hydration water surrounding protein or other hydrophilic macromolecular surfaces.[32] Next, when spin labeled PEG polymers are added to the dense coacervate fluid, their surface water diffusivities slow further, especially around the larger 17 or 20 kDa PEG surface (Figure 2). Given that we know from cryo-TEM of the presence of a bicontinuous phase with heterogeneities at the 100 nm and smaller length scale, it is most intuitive to suggest that the larger PEG molecules are getting entrapped in the smaller structures present in the dense coacervate fluid, and that the diffusivity is slowed due to molecular confinement felt by the PEG surface. Interestingly, the fraction of partitioning of the probes in the dense coacervate *vs* the dilute phase decreases from 1/2 for 4OH TEMPO to 1/6 for 4 kDa A SL-PEG to approximately 1/20 for both the 17 and 20 kDa SL-PEGs (Table 1). However, surprisingly, the cw EPR spectra show relatively high rotational diffusivity of the spin probes, presenting absolutely no difference in their rotational mobility in the dense coacervate fluid *vs* the dilute supernatant, whether probed by the smaller or bulkier SL-PEGs (Figure 3). This observation suggests that the heterogeneous bicontinuous polymer structure is controlling the partitioning of the PEG probes by their size, while the direct interaction between the polyelectrolyte constituents and the free spin probe or the spin label on the PEG probes is minimal. We note that the largest PEG concentration in the dense coacervate phase monitored by ONDP was merely 250 μM, which is not high enough to disrupt or affect the coacervate phase by osmotic pressure effects alone.

If so, what is the molecular and/or structural basis for the significant retardation of surface water diffusivity observed near the 20 and 17 kDa PEG surface in the dense complex coacervate phase compared to in the supernatant, given that we observe that the spin label mobility itself is unaltered according to the EPR line shape analysis, *i.e.*, suggesting that the physical confinement as detected by the spin probe is unaltered and minimal? In the absence of any measurable physical confinements felt by the PEG probes, the local solvent viscosity of the hydration water near the PEG probe itself must be increasing, implying an increase in the cohesive interaction of the local water network within the coacervate environment. Notably, this can only be achieved when PEG−water attraction is long-range and/or when PEG increases the cohesive interaction between neighboring water molecules that now encompasses a larger population of water than simply the first hydration layer of PEG. In other words, while the 17 and 20 kDa PEG do not strongly interact with the polyelectrolyte framework of the complex coacervate phase, they do strongly interact with the water pools of the complex coacervate nanophase, and so retard their solvent diffusivity. If unretarded water diffusivity is to reflect low cohesive water−water and low adhesive water−polymer energy within the dense complex coacervate fluid, a strongly retarded water diffusivity in the same environment implies stronger cohesive energy of the water phase within the complex coacervate fluid.

Structural Basis of Low Interfacial Tension. The cryo-TEM of the dense coacervate fluid in the absence of PEG shows a bicontinuous phase, as clearly discernible in Figure 4,

DOI: 10.1021/acsnano.5b07787
ACS Nano XXXX, XXX, XXX−XXX

which is consistent with previously reported results.[4] Surprisingly, when small concentrations of PEG probes on the order of 5% are added to the complex coacervate solution, the bicontinuous interconnected biphasic structure of the dense complex coacervate fluid is entirely abolished (Figure 4c). This implies that the subtle balance between weak polyelectrolyte−water and water−water interaction that is thought to be responsible for the occurrence of a bicontinuous fluid structure[10] is disturbed by the addition of small concentrations of PEG. Given that PEG−polyelectrolyte attraction has been shown to be minimal according to the EPR line shape analysis of spin labeled PEG that signifies high rotational mobility (Figure 3), it must be the water−water cohesive interaction that PEG is strengthening, as supported by the ODNP-derived diffusion retardation results (Figure 2b). This is further supported by the contrasting observation that in the presence of the small molecule spin probe, 4OH TEMPO, the dense complex coacervate phase still maintains the bicontinuous structure, consistent with the expectation that no corralling effect of hydration water is exerted by 4OH TEMPO (Figure 4b). The cryo-TEM experiments were repeated several times and the unobstructed bicontinuous structure in the presence of 4OH TEMPO, as well as the abolished bicontinuous structure in the presence of PEG, is observed repeatedly. We conclude that water within the dense complex coacervate phase is no longer strongly driven toward nanoscopic phase separation (phase separation into nanophases within the microphase-separated complex coacervate phase) from the polymer-rich fluid nanophase when PEG is added that strengthens water−water cohesive interaction.

The ultimate question is whether the highly dynamic bulk-like water diffusivity and the biphasic and bicontinuous structure are representative (and inter-related) properties of the dense complex coacervate phase, indicative of a low average cohesive energy that hence underlies the low interfacial tension of complex coacervate to water and other solid surfaces. If so, will altering this key property, as manifested in retarded water diffusivity achieved by the addition of PEG, alter the interfacial tension of the complex coacervate fluid? We perform the ultimate test by measuring the interfacial tension of the macrophase-separated complex coacervate fluid in the absence and presence of 20 kDa PEG, with the results presented in Figure 4d. First, we reproduce the expected low interfacial tension of about ∼0.18 ± 0.1 mN/m for the complex coacervate fluid that falls within the range of known values between 0.10 and 0.29, as derived from AFM measurements.[8,14] Crucially, we confirm a significant increase in interfacial tension to ∼1.46 ± 0.1 mN/m when only 250 μM of PEG is added to the coacervate fluid.[33] The increase in interfacial tension in the presence of the PEG confirms the expected relationship between the low interfacial energy and the bicontinuous phase of the coacervate.

Theoretical Basis of Low Interfacial Tension of a Biphasic and Bicontinuous Sponge Structure. Finally, we seek a theoretical basis for the low interfacial tension of the biphasic and bicontinuous coacervate phase. We specifically seek to understand the role of the water fraction and the water−water and polyelectreolyte complex−water interaction strength on the cohesive energy of the complex coacervate fluid phase, and consequently on its interfacial energy. The microscopic structure of the dense complex coacervate phase can be modeled as a water-filled sponge structure: the condensed polyelectrolyte framework of the sponge is made of nanophase separated polyelectrolyte complexes and pores filled with bulk-like water. Due to the local charge neutrality achieved in the polyelectrolyte complex framework, the polyelectrolyte complexes only weakly interact with the surrounding water, as we verified experimentally. In other words, the majority of water inside the pore behaves like bulk water, as verified experimentally by water diffusivity measurements within the dense complex coacervate phase.

This sponge-like structure can tune the interfacial tension between the dense complex coacervates and the dilute supernatant phase by altering the structural and physical property of the dense complex coacervate phase, and so altering its free energy. To model the free energy of this water-filled sponge-structured coacervate phase, we include the contribution of electrostatic correlation between the polyelectrolyte complexes and water, as well as between the polyelectrolyte complexes, besides the mixing free energy of the polyelectrolyte complexes consisting of polyanions and polycations and water according to the Flory−Huggins theory. So, when we model the sponge structure with a lattice model of total N sites, the free energy F of this sponge-like structure made of N nodes can be expressed as

$$\frac{F}{NkT} = \frac{\phi}{N_P}\ln\phi + (1-\phi)\ln(1-\phi) + \chi_{PW}\phi(1-\phi) - \alpha(\sigma\phi)^{3/2} \quad (1)$$

Here, ϕ is the concentration of the polyelectrolyte complexes, N_P is the effective length of the polymer complex, χ_{PW} is the interaction parameter between water and the polymer complex, σ is the effective charge density of the polymer complex, and α $\left(\alpha \equiv \frac{16\pi^2}{3}\left(\frac{l_B^3}{v}\right)^{1/2}\right)$ is the interaction strength between the polymer complexes. Here, l_B is the Bjerrum length $\left(l_B \equiv \frac{e^2}{4\pi\epsilon_0\epsilon kT}\right)$, ϵ is the dielectric constant of the polyelectrolyte phase or framework and $v$is the site volume. For simplicity, we define an interaction parameter between the polyelectrolyte complexes, η, as $\eta \equiv \alpha\sigma^{3/2}$. Thus, in eq 1, the first two terms represent the mixing entropy, the third term is the interaction between the polymer complex and water, and the last term is the electrostatic interaction between the polymer complexes. This electrostatic correlation term between the polyelectrolyte complexes is obtained from the self-energy calculation by the Debye−Huckel approximation[34] that assumes a uniform effective average charge density, σ. Thus, an increased water concentration within the coacervate phase implies a smaller effective polyelectrolyte complex concentration, ϕ, and thus a smaller average charge density of this phase, σ. Consequently, the interaction parameter between the polyelectrolyte complexes, η, effectively decreases with increasing water concentration. It is also assumed that the property of water inside the dense coacervate phase and the dilute supernatant phase is indistinguishable (which is consistent with our empirical observation), and thus that the water density does not change across the coacervate macro-phase boundary.

If we consider a planar interface, by setting the normal axis as the z-axis, the definition of the interfacial tension $\gamma = \frac{dF[\phi]}{dA}$, in which F represents the above-defined (eq 1) Flory−Huggins Gibbs free energy (consistent with the earlier definition of $\gamma \equiv (\partial G/\partial A)_{T,P}$) is translated into the following form with respect to the one-dimensional polymer density field $\phi(z)$,

DOI: 10.1021/acsnano.5b07787
ACS Nano XXXX, XXX, XXX−XXX

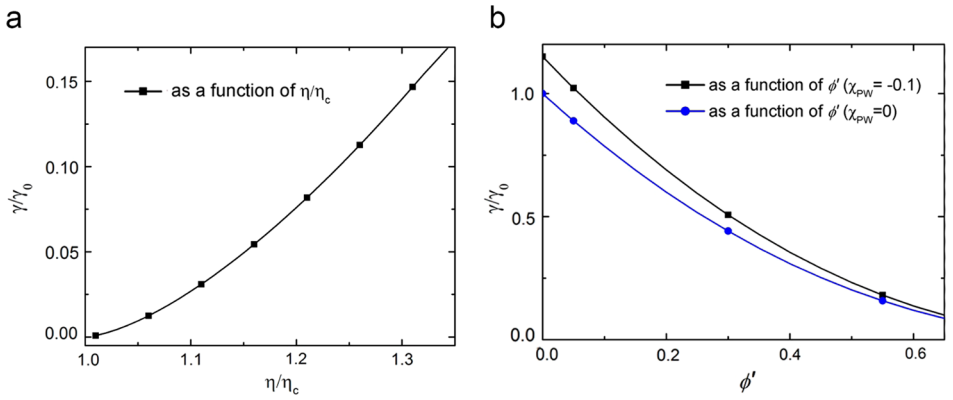

Figure 5. (a) Interfacial tension γ against interaction parameter η (eq 4) and (b) interfacial tension, γ, as a function of water concentration, ϕ', for χ_{PW} = 0, −0.1. Interfacial tension decreases with increasing water volume fraction, ϕ', decreasing water−polymer attraction, χ_{PW}, or increasing electrostatic self-energy, η, of polyelectrolyte complexes.

$$\gamma = \frac{kT}{v}\int_{-\infty}^{\infty} dz\left(f_0[\phi(z)] - f_0[\phi_0] + \frac{1}{2}B\left(\frac{d\phi}{dz}\right)^2\right) \quad (2)$$

Here, f_0 is the local part of free energy and ϕ_0 corresponds to the bulk polymer complex concentration. B is related to the thickness of the interface of the coacervate macro-phase boundary and is equal to $\frac{\sigma_0^2}{18\psi}$,[10] where σ_0 is the segmental length of the polymer. In the case when N is large, the ϕ and η at the critical point are $\phi_c \simeq \frac{1}{N_P(1-2\chi_{PW})}$ and $\eta_c \simeq \frac{8}{3}\phi_c^{3/2}\left\{\frac{1}{N_P\phi_c^2} - \frac{1}{(1-\phi_c)^2}\right\}$, respectively. Above the critical point, the free energy has two minima at densities corresponding to that of the respective phases. We expand the free energy near one of the free energy minima at ϕ_0, which corresponds to the bulk polymer density of the dense coacervate phase, and plug this into eq 2. Following the paper by Cahn and Hilliard,[35] we obtain the interfacial tension near the critical point for phase separation as,

$$\gamma = \frac{2\sqrt{2}}{3b}\left(\frac{\sigma_0^2}{36\phi_c}\right)^{1/2}(-2a)^{3/2} \quad (3)$$

where $a = \frac{1}{2!}\frac{\partial^2 f_0}{\partial\psi^2}$, and $b = \frac{1}{4!}\frac{\partial^4 f_0}{\partial\psi^4}$. In the limit where $|\chi_{PW}| \ll 1$ (this condition corresponds to the situation when the polymer−water interaction is smaller than kT), ϕ and η at the critical point are $\phi_c \simeq \frac{1}{N_P}(1+2\chi_{PW})$ and $\eta_c \simeq \frac{8}{3}N_P^{-(1/2)}(1-\chi_{PW})$. Then, $a = \frac{1}{2!}\frac{\partial^2 f_0}{\partial\psi^2} \simeq -(\eta/\eta_c - 1)(1-\chi_{PW})$, and $b = \frac{1}{4!}\frac{\partial^4 f_0}{\partial\psi^4} \simeq \frac{1}{4!}\frac{N_P^2}{2}$, which results in

$$\gamma = \gamma_0\left(1 - \frac{3}{2}\chi_{PW}\right) \quad (4)$$

This implies that the interfacial tension is larger when the polyelectrolyte−water interaction is attractive (making $\chi_{PW} < 0$) and displays a larger (negative) amplitude, and smaller when the polyelectrolyte−water attraction interaction is small, with γ equaling the zero interaction value, γ_0, when $\chi_{PW} < 0$. The dependence of the interfacial tension on the interaction parameter between the polyelectrolyte complexes, η, follows $\gamma_0 \propto (\eta/\eta_c - 1)^{3/2}$ as detailed in ref 10,[34] implying that the interfacial tension even more rapidly increases with increasing η (see Figure 5) than with (decreasing) χ_{PW}, and *vice versa*. This means that at increased salt concentration or well-matched polycation and polyanion complexation when optimal charge screening of the polyelectrolyte complex is achieved, the weakened polymer−water interaction as reflected in smaller $|\chi_{PW}|$ values will depress the interfacial tension, while the weakened interpolymer complex interaction as reflected in decreased η/η_c values will even more steeply depress the interfacial tension of the complex coacervate fluid, as shown in Figure 5.

The effect of the internal structure of the dense complex coacervate phase is considered at the zeroth order level. Instead of considering spatial inhomogeneity of the polymer complex density within the dense complex coacervate phase, we assumed that the density of the polymer complex is reduced by the amount of water in the dense phase, and thus accordingly the average effective charge density of the dense complex coacervate phase reduced. The computed dependence of the interfacial tension, γ, on the water concentration, $\phi' = 1 - \phi$ that originates from the decreased effective interaction parameter, η, between the polyelectrolyte complexes is shown in Figure 5. Clearly, increasing water concentration, ϕ', decreases γ, while the overall γ amplitude is depressed as $|\chi_{PW}|$ decreases and approaches 0. Taken together, this theoretical exercise illustrates that the large water population (large ϕ') found within the bicontinuous structure that is weakly bound to the polyelectrolyte complexes (small $|\chi_{PW}|$ value), together with weak interactions between the polyelectrolyte complexes (small η/η_c) are all essential factors in rationalizing the exceptionally low interfacial tension measured of the dense complex coacervate phase that was found to display a sponge-like internal structure filled with freely diffusing, bulk-like, water. We note that our analysis based on the Flory−Huggins theory within the Debye−Huckel (DH) approximation may be an oversimplification of the system at hand by ignoring the strong coupling effects of electrostatic interaction and the configurational change of the polyelectrolytes. In addition, the effect of water can only be considered phenomenologically in this model. Nevertheless, these approaches have been successful in explaining the qualitative behaviors of complex coacervation.[10,36]

DOI: 10.1021/acsnano.5b07787
ACS Nano XXXX, XXX, XXX−XXX

CONCLUSION

Employing a combination of innovative experimental tools, we make the discovery that the dense complex coacervate fluid is a phase displaying a bicontinuous and biphasic fluid structure within this macrophase, displaying nanophase separation at length scales of 100 nm and smaller, in which one is a bulk-like water nanophase and the other a polyelectrolyte-rich nanophase. The bulk-like water phase is shown to occupy 50% (v/v) of the dense complex coacervate fluid, in which an exceptionally low cohesive energy of the dense complex coacervate fluid based on weak interactions between water−polyelectrolyte complexes and water−water is found to be the molecular basis of the low interfacial tension of the dense complex coacervated fluid, found with respect to virtually any surface in an aqueous medium. We propose that the weakening of a contiguous and strong hydrogen bond network of water within the complex coacervate phase is due to weakened interactions between the polyelectrolyte complexes and water. By the same logic, we show that the addition of PEG that is known to corral an extended hydration shell strengthens the water network within the dense complex coacervate phase, as manifested in retarded water diffusivity measured within the complex coacervate fluid. The addition of PEG consequently leads to an increased interfacial tension of the dense complex coacervate to the water phase. A theoretical model that describes the relationship between the low interfacial tension of a coacervate fluid and the weak cohesive energy of a complex fluid with a sponge-like structure is provided. A sponge-like fluid structure is formed when the water−water cohesive and polyelectrolyte−water attractive energy is very small, which in turn requires the polyelectrolyte complexes to display an effectively charge-neutralized and less hydrophilic surface, that is still hydrated. Within this sponge-like structure model for the complex coacervate fluid, a low electrostatic correlation energy is achieved with an increasing water-filled pore fraction of the sponge structure that effectively reduces the polymer concentration and/or by the addition of salt or other means that decrease the effective surface charges on the surface of the polyelectrolyte complexes. This study offers a rationale and physical basis for the exceptionally low interfacial tension of complex coacervate fluid, as well as a design principle for a fluid material with low interfacial tension that is an important base property for underwater adhesives.

METHODS

Materials. Recombinant mfp-1 was prepared as previous described.[24,25] Hyaluronic acid (35 kDa) was purchased from Lifecore Biomedical (Chaska, MN,). Spin probe 4-hydroxy TEMPO was purchased from Sigma-Aldrich (St. Louis, MO). Small spin labeled PEG poly(ethylene glycol)-bis-TEMPO (extent of labeling: 0.25−0.75 mmol/g) was also purchased from Sigma-Aldrich. Large spin labeled PEG, 20 kDa linear PEG, and 17 kDa 6 arms PEG were prepared by attaching 4-carboxy TEMPO (Sigma-Aldrich) to polyethylene glycol through Steglich esterification reaction. Experimental details of Steglich esterification are shown as below: PEG (1 g, 0.05 mmol 20k linear PEG, or 250 mg, 0.0147 mmol 17k 6 arms PEG), 4-carboxy-TEMPO (110 mg, 0.55 mmol), and 4-dimethylaminopyridine (4 mg, 0.04 mmol) dissolved in dry dichloromethane (10 mL) were added to dicyclohexylcarbodiimide (113 mg, 0.55 mmol) under N_2 atmosphere. After 2 days of stirring at room temperature, the mixture was filtered, the solvent was removed *in vacuo*, and the residue was dialyzed in 3 kDa molecular weight cutoff (MWCO) cellulose membranes against distilled water. The product was obtained by lyophilization. Spin labeling efficiency (>90%) was determined by double integration of the EPR signal. Spin labeling of mfp-1 was carried out by addition of MTSL (*S*-(2,2,5,5-tetramethyl-2,5-dihydro-1*H*-pyrrol-3-yl)-methylmethanesulfonothioate) in 2-fold excess, resulting in the quantitative functionalization of mfp1 at its single cysteine residue (Figure S2).

Preparation of Dense and Dilute Coacervates with Spin. Complex coacervates of mfp-1 and HA were prepared by addition of HA into protein solution at varying molar ratios: 2% (w/v) mfp1 and 2% (w/v) HA were dissolved into 10 mM sodium acetate buffer (pH 5.0). The condition of pH 5.0 and 10 mM acetate buffer was employed, as pH 5.0 was found to be an appropriate pH to form complex coacervation, given that the pK_a value of COOH in HA is 2.9,[37,38] and because the use of low salt concentration of 10 mM acetic acid buffer was important when using the pendant drop method to measure the interfacial energy. In addition, most of the previous studies on coacervate systems with recombinant MAP[37,39,40] were performed under this condition. The total polymer concentration was fixed at 2% (w/v) for all combinations of mfp-1 and HA. Complex coacervation of the two polyelectrolytes was measured turbidimetrically at 600 nm by UV−vis spectrophotometry. The relative turbidity is defined as $\ln(T/T_0)$ where T and T_0 are light transmittance with and without sample, respectively.[4] The zeta potential of coacervates was measured by a Malvern 3000 Zetasizer instrument at 25 °C. The instrument uses a 10 mW He−Ne laser operating at 632.8 nm. Changes in the zeta potential of complex coacervate of mfp-1/HA were investigated by incremental additions wt % of HA at pH 5.0. Concentration of mfp-1 and HA in dilute phase and dense phase was measured by amino acid analyze (S4300, SYKAM, Germany). Both the dilute and coacervate phase were hydrolyzed in a 6 M HCl solution of 5% water-saturated phenol at 110 °C and under argon for 24 h. Afterward, the samples were flash-evaporated at 60 °C under vacuum and washed until dry, twice with 1 mL of DI water, and then again twice with 1 mL of methanol. The samples were then resuspended in 250−500 μL of dilution buffer and injected to a ninhydrin-based Amino Acid Analyzer (SYKAM System S4300). Since the *N*-acetyl-D-glucosamine units of hyaluronic acid yield D-glucoamine after acid hydrolysis as described, D-glucosamine was used for the quantification of HA. For ODNP and EPR measurements, mfp-1/HA complex coacervates were prepared by mixing mfp-1 and HA solution with the mass ratio of 55:45 with the total polymer concentration of 2% (w/v). After 1 h equilibration time, spin probes (3 times the final concentration) were introduced into mfp-1/HA mixture and continued to equilibrate overnight (store at 4 °C). Two phases were formed after 2000*g* centrifugation for 10 min. The dilute phase can be also physically separated from the dense phase after 2 days at 4 °C storage, and right before ODNP and EPR measurements. Both dilute phase and dense phase were measured individually by ODNP and EPR.

Overhauser Dynamic Nuclear Polarization (ODNP). ^{1}H ODNP experiments were performed at a 0.35 T electromagnet, operating at 14.8 MHz ^{1}H Larmor frequency and at 9.8 GHz electron Larmor frequency. A 3.5 μL sample was loaded in a 0.02 in. I.D. PTFE tube (VICI Valco Instruments Co. Inc.) and sealed at both ends with bee wax. The PTFE tube was mounted on a home-built NMR probe with a U-shaped NMR coil. Dry air was streamed through the NMR probe at 15 SCFH, and all spectra were acquired at 298 K.

Electron Paramagnetic Resonance (EPR). CW EPR spectra were measured on a Bruker EMX X-band spectrometer equipped with a ER4123D dielectric resonator. Samples were irradiated at 9.8 GHz with the center field set at 3400 G and sweep width of 100 G. The field modulation amplitude was kept below 0.2 times the center peak line width to acquire the intrinsic EPR line shapes and amplitudes. Dry air was streamed through the cavity at 15 SCFH, and all spectra were acquired at 298 K.

Preparation of Cyro-TEM. Cryo-TEM samples of mfp-1/HA complex coacervates were prepared by mixing mfp-1 and HA solution with the mass ratio of 55:45. After 1 h equilibration time, 2000*g* centrifugation for 10 min was perform to have two phases separation. The 5 μL of dense phase of complex coacervates was transferred to a B-type aluminum planchette (Technotrade International). The

DOI: 10.1021/acsnano.5b07787
ACS Nano XXXX, XXX, XXX−XXX

coacervate samples were then covered with the flat side of another B-type planchette and were rapidly frozen in a Bal-Tec HPM 010 high-pressure freezer (Boeckeler Instruments). After freeze substitution for 5 days at −80 °C in anhydrous acetone containing 2% OsO_4, the samples were warmed to room temperature over 2 days (24 h from −80 to −20 °C, 20 h from −20 to 4 °C, 4 h from 4 to 20 °C). The structure of the phase separated complex coacervation fluid was fixed with osmium before washing it with acetone. Therefore, acetone is not expected to perturb the structural features imaged. After 3 washes with anhydrous acetone, the complex coacervate samples were embedded in a graduated Epon resin (Ted Pella Inc.) dilution in acetone (5, 15, 25, 50, 75, and 100% (v/v)) over 3 days. After polymerization in a 60 °C oven for 24 h, the resin was cut into 200 nm-sections using Leica EM UC7 (Germany) and applied onto copper grids. All TEM images were recorded using a transmission electron microscope (JEOL, JEM 1011 Tokyo, Japan).

Pendant Drop Method. The interfacial energy was measured by the pendant drop method which measures the boundary tension of the pendant drop in water.[41] Since there are no variables such as the viscosity or inertia, the Laplace equation can be applied in response to the surface and gravitational energy to obtain the interfacial energy. With the use of the Drop shape Analyzer (DSA100) from KRUSS (Hamburg, Germany), image analysis with Young Laplace drop shape analysis was done to obtain the interfacial energy. The pendant droplet image was captured by the build-in high-speed camera, and with the use of the DSA3 software, the interfacial energy was calculated after manual input of substance density, magnification scale and calibration object dimension.

Cryo-TEM Image Anaylsis. From the cryo-TEM image, we use image processing to determine the percentage of white spot (water) and black structure. Any colors in any image are usually represented by color code ranging from 0 to 255, where 0 represents black color and 255 represents white color. The image processing algorithm will calculate the number of pixel covered by the black and white spot on the image by counting the total number color code of 0 and 255, respectively. For example, suppose the image processing algorithm detected [0,0,255,255,0,0] from a given image. This means the total black pixel and white pixel are 3 and 2, respectively. In terms of percentage, we have 60% black and 40% white. With this algorithm, the image processing will count the number of 0 and 255 from the cyro-TEM image and the results are represented in percentage on a bar graph.

ASSOCIATED CONTENT

Supporting Information

The Supporting Information is available free of charge on the ACS Publications website at DOI: 10.1021/acsnano.5b07787.

Additional experimental results (PDF)

AUTHOR INFORMATION

Corresponding Authors

*E-mail: ysjho1@ibs.re.kr.
*E-mail: songi@chem.ucsb.edu.
*E-mail: dshwang@postech.ac.kr.

Author Contributions

#K.-Y.H. and H.Y.Y. contributed equally.

Notes

The authors declare no competing financial interest.

ACKNOWLEDGMENTS

This material is based upon work supported by the National Research Foundation of Korea (NRF-2016M1A5A1027592, NRF- 2014R1A6A1031189, NRF-2011-0008261), and the Marine Biotechnology Program (Marine BioMaterials Research Center, D11013214H480000110), funded by the Ministry of Oceans and Fisheries, Korea. This work was partially supported by the Institute for Basic Science, project code IBS-R020-D1. This research was supported by the U.S. National Science Foundation (NSF) through the MRSEC Program DMR-1121053 (MRL-UCSB) for all authors. S.H. also would like to acknowledge support by the 2011 NIH Innovator Award.

REFERENCES

(1) Waite, J. H. Evidence for a Repeating 3,4-dihydroxyphenylalanine- and Hydroxyproline-Containing Decapeptide in the Adhesive Protein of the Mussel, Mytilus edulis L. *J. Biol. Chem.* **1983**, *258*, 2911−2915.

(2) Lee, H.; Scherer, N. F.; Messersmith, P. B. Single-Molecule Mechanics of Mussel Adhesion. *Proc. Natl. Acad. Sci. U. S. A.* **2006**, *103*, 12999−13003.

(3) Zhao, H.; Sun, C.; Stewart, R. J.; Waite, J. H. Cement Proteins of the Tube-building Polychaete Phragmatopoma californica. *J. Biol. Chem.* **2005**, *280*, 42938−42944.

(4) Hwang, D. S.; Zeng, H.; Srivastava, A.; Krogstad, D. V.; Tirrell, M.; Israelachvili, J. N.; Waite, J. H. Viscosity and Interfacial Properties in a Mussel-Inspired Adhesive Coacervate. *Soft Matter* **2010**, *6*, 3232−3236.

(5) de Jong, H. G. B. Die Koazervation und ihre Bedeutung für die Biologie. *Protoplasma* **1932**, *15*, 110−173.

(6) de Kruif, C. G.; Weinbreck, F.; de Vries, R. Complex Coacervation of Proteins and Anionic Polysaccharides. *Curr. Opin. Colloid Interface Sci.* **2004**, *9*, 340−349.

(7) Winslow, B. D.; Shao, H.; Stewart, R. J.; Tresco, P. A. Biocompatibility of Adhesive Complex Coacervates Modeled after the Sandcastle Glue of Phragmatopoma Californica for Craniofacial Reconstruction. *Biomaterials* **2010**, *31*, 9373−9381.

(8) Spruijt, E.; Sprakel, J.; Cohen Stuart, M. A.; van der Gucht, J. Interfacial Tension Between a Complex Coacervate Phase and Its Coexisting Aqueous Phase. *Soft Matter* **2010**, *6*, 172−178.

(9) Priftis, D.; Farina, R.; Tirrell, M. Interfacial Energy of Polypeptide Complex Coacervates Measured *via* Capillary Adhesion. *Langmuir* **2012**, *28*, 8721−8729.

(10) Qin, J.; Priftis, D.; Farina, R.; Perry, S. L.; Leon, L.; Whitmer, J.; Hoffmann, K.; Tirrell, M.; de Pablo, J. J. Interfacial Tension of Polyelectrolyte Complex Coacervate Phases. *ACS Macro Lett.* **2014**, *3*, 565−568.

(11) Riggleman, R. A.; Kumar, R.; Fredrickson, G. H. Investigation of the Interfacial Tension of Complex Coacervates Using Field-Theoretic Simulations. *J. Chem. Phys.* **2012**, *136*, 024903.

(12) Kizilay, E.; Kayitmazer, A. B.; Dubin, P. L. Complexation and Coacervation of Polyelectrolytes with Oppositely Charged Colloids. *Adv. Colloid Interface Sci.* **2011**, *167*, 24−37.

(13) Perry, S. L.; Li, Y.; Priftis, D.; Leon, L.; Tirrell, M. The Effect of Salt on the Complex Coacervation of Vinyl Polyelectrolytes. *Polymers* **2014**, *6*, 1756−1772.

(14) Lim, S.; Moon, D.; Kim, H. J.; Seo, J. H.; Kang, I. S.; Cha, H. J. Interfacial Tension of Complex Coacervated Mussel Adhesive Protein According to the Hofmeister Series. *Langmuir* **2014**, *30*, 1108−1115.

(15) Spruijt, E.; Sprakel, J.; Lemmers, M.; Stuart, M. A. C.; van der Gucht, J. Relaxation Dynamics at Different Time Scales in Electrostatic Complexes: Time-Salt Superposition. *Phys. Rev. Lett.* **2010**, *105*, 208301.

(16) Priftis, D.; Tirrell, M. Phase Behaviour and Complex Coacervation of Aqueous Polypeptide Solutions. *Soft Matter* **2012**, *8*, 9396−9405.

(17) Kausik, R.; Srivastava, A.; Korevaar, P. A.; Stucky, G.; Waite, J. H.; Han, S. Local Water Dynamics in Coacervated Polyelectrolytes Monitored Through Dynamic Nuclear Polarization-Enhanced 1H NMR. *Macromolecules* **2009**, *42*, 7404−7412.

(18) Bohidar, H.; Dubin, P. L.; Majhi, P. R.; Tribet, C.; Jaeger, W. Effects of Protein−Polyelectrolyte Affinity and Polyelectrolyte Molecular Weight on Dynamic Properties of Bovine Serum Albumin−Poly(diallyldimethylammonium chloride) Coacervates. *Biomacromolecules* **2005**, *6*, 1573−1585.

DOI: 10.1021/acsnano.5b07787
ACS Nano XXXX, XXX, XXX−XXX

(19) Du, X.; Seeman, D.; Dubin, P. L.; Hoagland, D. A. Nonfreezing Water Structuration in Heteroprotein Coacervates. *Langmuir* **2015**, *31*, 8661−8666.
(20) Song, J.; Allison, B.; Han, S. Local Water Diffusivity as a Molecular Probe of Surface Hydrophilicity. *MRS Bull.* **2014**, *39*, 1082−1088.
(21) Armstrong, B. D.; Han, S. Overhauser Dynamic Nuclear Polarization to Study Local Water Dynamics. *J. Am. Chem. Soc.* **2009**, *131*, 4641−4647.
(22) Kausik, R.; Han, S. Ultrasensitive Detection of Interfacial Water Diffusion on Lipid Vesicle Surfaces at Molecular Length Scales. *J. Am. Chem. Soc.* **2009**, *131*, 18254−18256.
(23) Wu, J.; Chen, S. Investigation of the Hydration of Nonfouling Material Poly(ethylene glycol) by Low-Field Nuclear Magnetic Resonance. *Langmuir* **2012**, *28*, 2137−2144.
(24) Ortony, J. H.; Hwang, D. S.; Franck, J. M.; Waite, J. H.; Han, S. Asymmetric Collapse in Biomimetic Complex Coacervates Revealed by Local Polymer and Water Dynamics. *Biomacromolecules* **2013**, *14*, 1395−1402.
(25) Zeng, H.; Hwang, D. S.; Israelachvili, J. N.; Waite, J. H. Strong Reversible Fe3+-Mediated Bridging Between DOPA-Containing Protein Films in Water. *Proc. Natl. Acad. Sci. U. S. A.* **2010**, *107*, 12850−12853.
(26) Kim, S.; Huang, J.; Lee, Y.; Dutta, S.; Yoo, H. Y.; Jung, Y. M.; Jho, Y.; Zeng, H.; Hwang, D. S. Complexation and Coacervation of Like-Charged Polyelectrolytes Inspired by Mussels. *Proc. Natl. Acad. Sci. U. S. A.* **2016**, *113*, E847−E853.
(27) Krogstad, D. V.; Choi, S.-H.; Lynd, N. A.; Audus, D. J.; Perry, S. L.; Gopez, J. D.; Hawker, C. J.; Kramer, E. J.; Tirrell, M. V. Small Angle Neutron Scattering Study of Complex Coacervate Micelles and Hydrogels Formed from Ionic Diblock and Triblock Copolymers. *J. Phys. Chem. B* **2014**, *118*, 13011−13018.
(28) Kizilay, E.; Dinsmore, A. D.; Hoagland, D. A.; Sun, L.; Dubin, P. L. Evolution of Hierarchical Structures in Polyelectrolyte-Micelle Coacervates. *Soft Matter* **2013**, *9*, 7320−7332.
(29) Menger, F. M.; Peresypkin, A. V.; Caran, K. L.; Apkarian, R. P. A Sponge Morphology in an Elementary Coacervate. *Langmuir* **2000**, *16*, 9113−9116.
(30) Hopp, T. P.; Woods, K. R. Prediction of Protein Antigenic Determinants from Amino Acid Sequences. *Proc. Natl. Acad. Sci. U. S. A.* **1981**, *78*, 3824−3828.
(31) Remsing, R. C.; Xi, E.; Vembanur, S.; Sharma, S.; Debenedetti, P. G.; Garde, S.; Patel, A. J. Pathways to Dewetting in Hydrophobic Confinement. *Proc. Natl. Acad. Sci. U. S. A.* **2015**, *112*, 8181−8186.
(32) Franck, J. M.; Pavlova, A.; Scott, J. A.; Han, S. Quantitative CW Overhauser Effect Dynamic Nuclear Polarization for the Analysis of Local Water Dynamics. *Prog. Nucl. Magn. Reson. Spectrosc.* **2013**, *74*, 33−56.
(33) Song, B.; Springer, J. Determination of Interfacial Tension from the Profile of a Pendant Drop Using Computer-Aided Image Processing: 1. Theoretical. *J. Colloid Interface Sci.* **1996**, *184*, 64−76.
(34) Potemkin, I. I.; Limberger, R. E.; Kudlay, A. N.; Khokhlov, A. R. Rodlike Polyelectrolyte Solutions: Effect of the Many-Body Coulomb Attraction of Similarly Charged Molecules Favoring Weak Nematic Ordering at Very Small Polymer Concentration. *Phys. Rev. E: Stat. Phys., Plasmas, Fluids, Relat. Interdiscip. Top.* **2002**, *66*, 011802.
(35) Cahn, J. W.; Hilliard, J. E. Free Energy of a Nonuniform System. I. Interfacial Free Energy. *J. Chem. Phys.* **1958**, *28*, 258−267.
(36) Kudlay, A.; Olvera de la Cruz, M. Precipitation of Oppositely Charged Polyelectrolytes in Salt Solutions. *J. Chem. Phys.* **2004**, *120*, 404−412.
(37) Miller, D. R.; Das, S.; Huang, K.-Y.; Han, S.; Israelachvili, J. N.; Waite, J. H. Mussel Coating Protein-Derived Complex Coacervates Mitigate Frictional Surface Damage. *ACS Biomater. Sci. Eng.* **2015**, *1*, 1121−1128.
(38) Waite, J. H.; Andersen, N. H.; Jewhurst, S.; Sun, C. Mussel Adhesion: Finding the Tricks Worth Mimicking. *J. Adhes.* **2005**, *81*, 297−317.
(39) Lim, S.; Choi, Y. S.; Kang, D. G.; Song, Y. H.; Cha, H. J. The Adhesive Properties of Coacervated Recombinant Hybrid Mussel Adhesive Proteins. *Biomaterials* **2010**, *31*, 3715−3722.
(40) Ortony, J. H.; Choi, S.-H.; Spruell, J. M.; Hunt, J. N.; Lynd, N. A.; Krogstad, D. V.; Urban, V. S.; Hawker, C. J.; Kramer, E. J.; Han, S. Fluidity and Water in Nanoscale Domains Define Coacervate Hydrogels. *Chem. Sci.* **2014**, *5*, 58−67.
(41) Stauffer, C. E. The Measurement of Surface Tension by the Pendant Drop Technique. *J. Phys. Chem.* **1965**, *69*, 1933−1938.

DOI: 10.1021/acsnano.5b07787
ACS Nano XXXX, XXX, XXX−XXX